

## CHAPTER 4

### RESULTS AND DISCUSSION

#### 4.1 Crystalline Phase Analysis

##### 4.1.1 Wide Angle X-ray diffraction (WAXD) studies

##### 4.1.1.1 Compressed films

The effect of  $\beta$ -nucleator (Permanent Red E3B) on the crystalline phase of compressed films containing various amount of  $\beta$ -nucleators in a range of 0.0001-0.01% by weight was investigated by wide angle x-ray diffraction (WAXD). Table 4.1 show all  $\beta$ -nucleator-PP samples studied with details of their compositions and preparations.

Table 4.1 The  $\beta$ -nucleated PP Pellet with various  $\beta$ -nucleator content and different preparation method.

Sample	Type	$\beta$ nucleator(E3B) concentration	Mixing prior to pelletization
Pure PP	PP	PP 100%	-
PP-E3B	P0.0001	PP+0.0001%Permanent Red E3B	Mechanical Blending
	P0.001	PP+0.001%Permanent Red E3B	
	P0.01	PP+0.01%Permanent Red E3B	
PP-masterbatch	M0.0001	PP + master batch (0.0001% E3B)	Internal mixing (masterbatch)
	M0.001	PP + master batch (0.001% E3B)	
	M0.01	PP + master batch (0.01% E3B)	

Figure 4.1 shows the WAXD results for pure PP,PP-E3B and PP-masterbatch containing 0.0001% , 0.001% , and 0.01% of E3B. All these compressed film samples were prepared using the same condition of 210<sup>o</sup>C molding temperature, 15 tons pressure and 5 min cooling time, as described in section 3.2.3

It is clearly seen from these WAXD results that for pure PP sharp diffraction peak take place at the angles ( $2\theta$ ) of  $14.2^\circ$ ,  $17.0^\circ$ , and  $18.8^\circ$ . These pattern conform the characteristics of monoclinic  $\alpha$  iPP structure. On the other hand, PP with Permanent Red E3B samples exhibit sharp peaks at the angles ( $2\theta$ ) of  $16.2^\circ$ . These diffractograms conform characteristics of hexagonal  $\beta$  iPP structure. The comparison of the pattern of diffractograms indicates that pure PP crystallizes in the  $\alpha$  form. For PP with Permanent Red,  $\beta$ -phase are obviously present in the PP sample. The  $\beta$  phase content was determined by ratio of the intensities of the main  $\beta$  300 peak ( $2\theta = 16.2^\circ$ ) to that of  $\alpha_{110}$  peak ( $2\theta = 14.20^\circ$ )  $\alpha_{040}$  peak ( $2\theta = 17.0^\circ$ ) and  $\alpha_{130}$  peak ( $2\theta = 18.8^\circ$ ), as  $H\beta / [H\beta + H\alpha]$ .

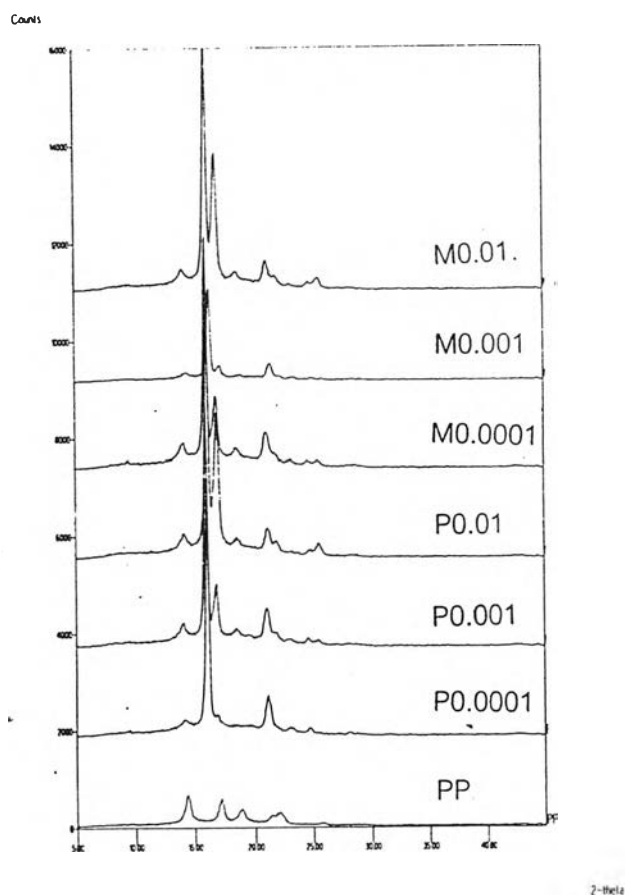


Figure 4.1 The wide angle X-ray diffraction scans for compressed films of iPP PP, P0.0001, P0.001, P0.01, M0.0001, M0.001, M0.01 ( see Table 4.1 for detailed sample description )

From Figure 4.2, it can be seen that in the case of iPP-Mater batch( M0.0001-M0.010 ), the  $\beta$  phase content increases with an increase of  $\beta$ -nucleator (E3B) up to about 0.001% and then decreases with the increase concentration of the  $\beta$ -nucleator. On the other hand, in the case of PP-E3B (P0.0001-P0.01) , the  $\beta$  phase content is maximum at 0.0001% E3B and then decreases with increasing concentration of the  $\beta$ -nucleator. These finding clearly suggest that the selected Permanent Red E3B is an effective  $\beta$  nucleator for PP. With a use of only 0.0001% E3B in PP-E3B blend compressed film, high  $\beta$  phase content as indicated by the  $k_x$  of 0.91 can be obtained.

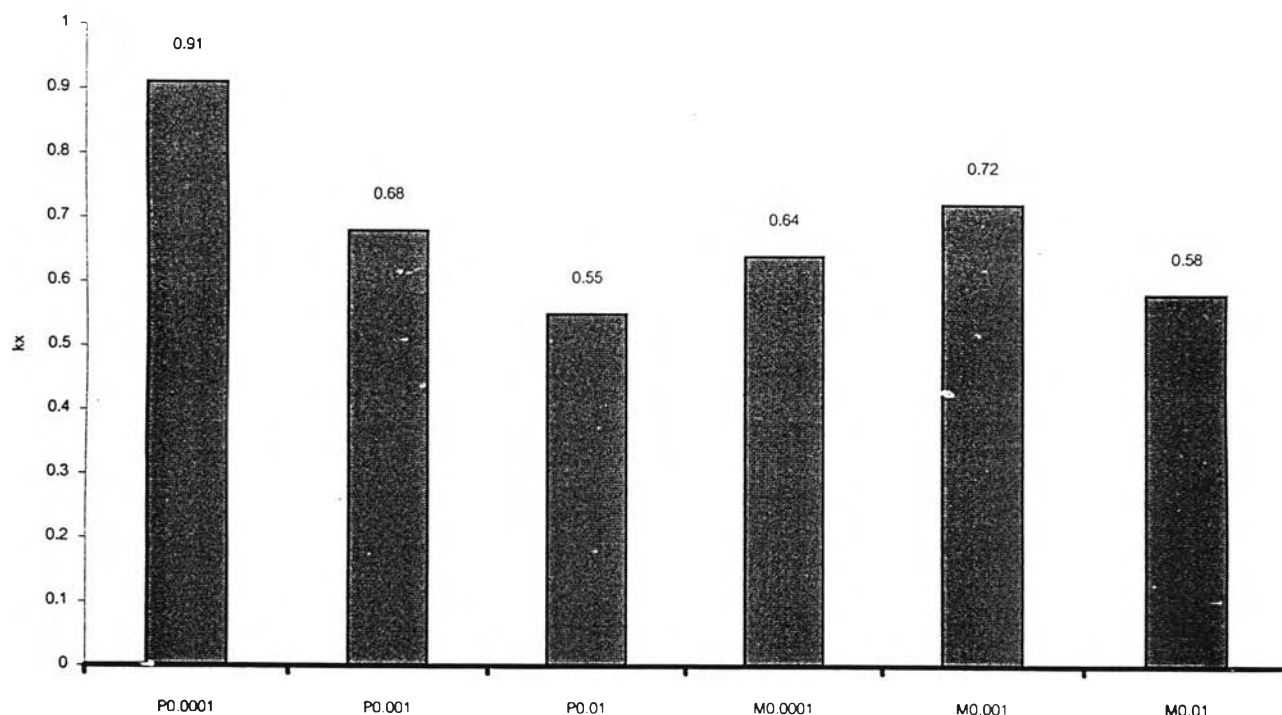


Figure 4.2 shows the variation of  $\beta$ -phase content with the concentration of  $\beta$ -nucleators in compressed films prepared from PP-nucleator mechanical blends or PP-masterbatch.

#### 4.1.1.2 Extruded films

The effect of  $\beta$ -nucleator (Permanent Red E3B) on the crystalline phase of extruded films containing variation of  $\beta$ -nucleator contents were also investigated by wide angle X-ray diffraction (WAXD). Figure 4.3 shows the WAXD scans for PP, P0.0001, P0.001, P0.01, M0.0001, M0.001, and M0.01. All diffractograms are determined by two diffused reflections centered at  $2\theta=14.8^\circ$  and  $21.3^\circ$  which are characteristic of the smectic PP. This observation may suggest that the E3B used with a low concentration in a range of 0.0001-0.01% can not nucleate  $\beta$  phase in extruded film production. However, as reported by several investigators<sup>38</sup>, the smectic form present in produced extruded films may imply partial ordered structure of the PP macromolecules. The structure form of the smectic iPP is still inconclusive, whether this form is mainly composed of  $\alpha$  iPP crystal or small crystals of the  $\beta$  iPP.

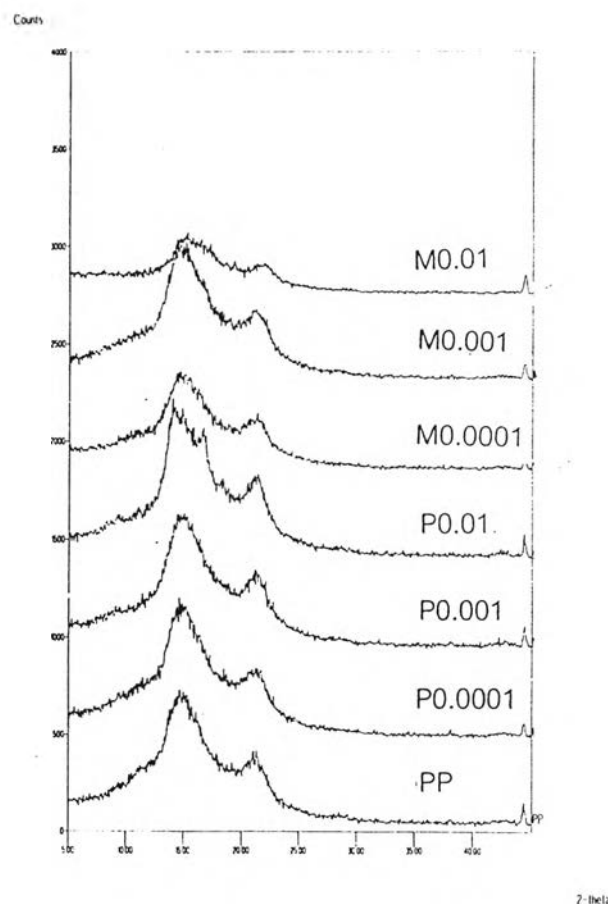


Figure 4.3 The wide angle X-ray diffraction scans for extruded films of iPP PP, P0.0001, P0.001, P0.01, M0.0001, M0.001, M0.01.



## 4.1.2 Differential Scanning Calorimetry (DSC) studies

### 4.1.2.1 Compressed films

The melting thermogram of PP-E3B and PP-masterbatch compressed films can be seen from the DSC scan as shown in Figure 4.4. The endotherm peak at 160°C is due to the melting of  $\alpha$ -form. This peak is evident as for pure PP sample. The endotherm peak at 148°C is due to the melting of  $\beta$ -form polypropylene. It has been suggested that the apparent endotherm between  $\beta$  and  $\alpha$  melting endotherms could arise by the exothermic event of the recrystallization of melted  $\beta$ -form into the  $\alpha$ -form<sup>58</sup>. The comparison of the melting peak of  $\beta$ -form PP-masterbatch compressed films (M0.0001-M0.01) reveals that, the height of  $\beta$ -melting peak increases with increasing  $\beta$ -nucleator from 0.0001 to 0.001 %. However a decrease of  $\beta$ -form melting peak height can be observed in the case of M0.01. In the case of PP-E3B compressed films, the height of  $\beta$ -melting peak is maximum at 0.0001% by wt of E3B then decreases with increasing concentration of the  $\beta$ -nucleator. These observations on the  $\beta$ -melting peak height agree well with the  $k_x$  value obtained from X-ray diffractograms. Overall results indicate that the Permanent Red E3B is an effective nucleator for the  $\beta$  phase, however its efficiency in generating  $\beta$ -crystal can be affected by incorporation process of the E3B into the PP resin. It is well known that different incorporation or mixing process of dyes or additives can result in different degree of dispersion and distribution of such additives.

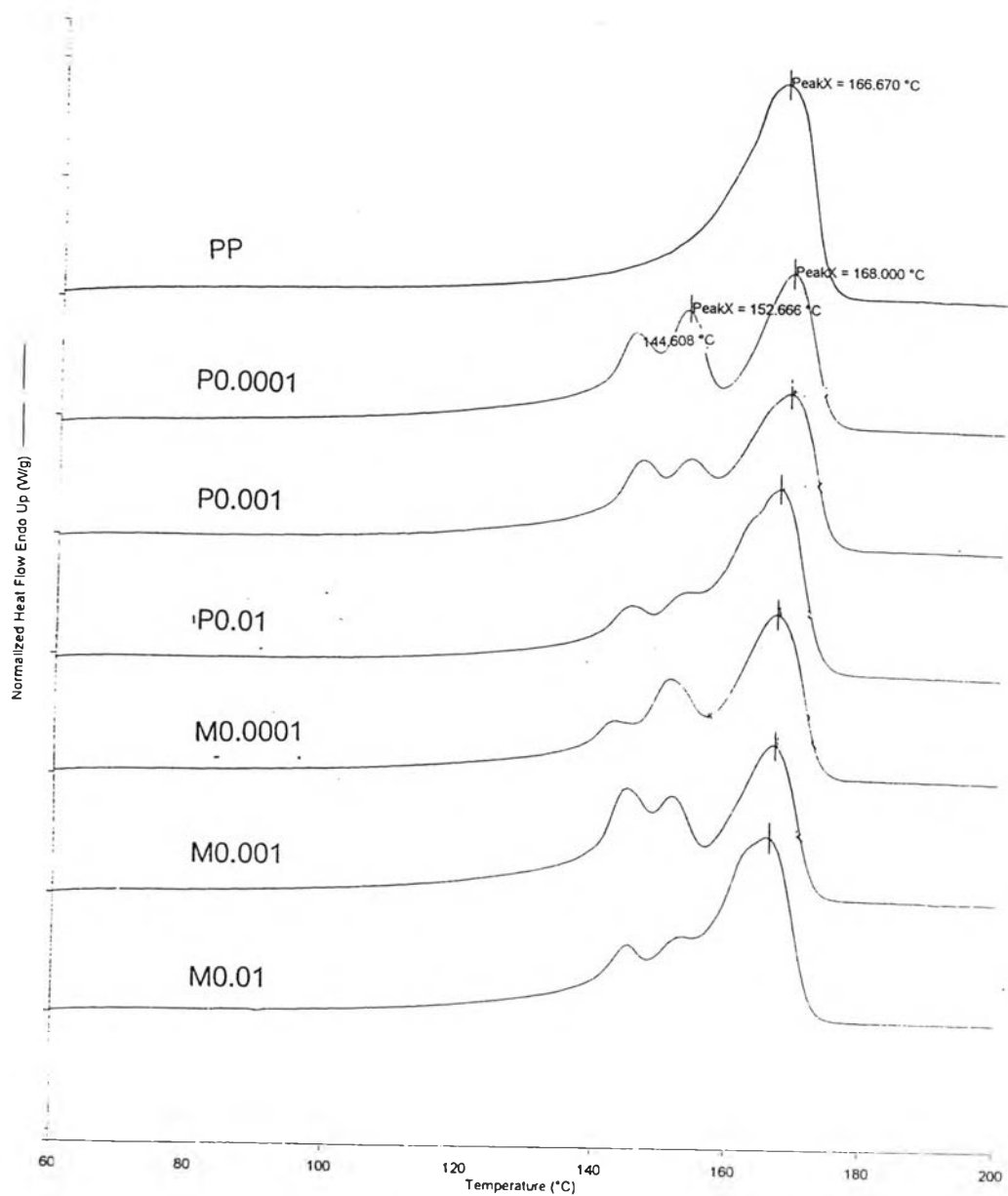


Figure 4.4 The DSC melting thermogram of compressed films PP, P0.0001, P0.001, P0.01, M0.0001, M0.001, M0.01

The crystallization thermogram of PP-E3B and PP-masterbatch compressed films can be seen from the DSC result as shown in Figure 4.5. The comparison of crystallization peak of PP, PP-E3B and PP-masterbatch, indicate that the crystallization temperature(  $T_c$  ) of PP is lower than that of PP containing the  $\beta$ -nucleator. In both PP-E3B and PP-masterbatch samples, the observed crystallization peaks tend to shift to higher temperature with the increasing concentration of  $\beta$ -nucleator. These result shows that upon cooling sample containing a higher content of E3B favors the crystallization process, as compared to that with lower E3B loading.

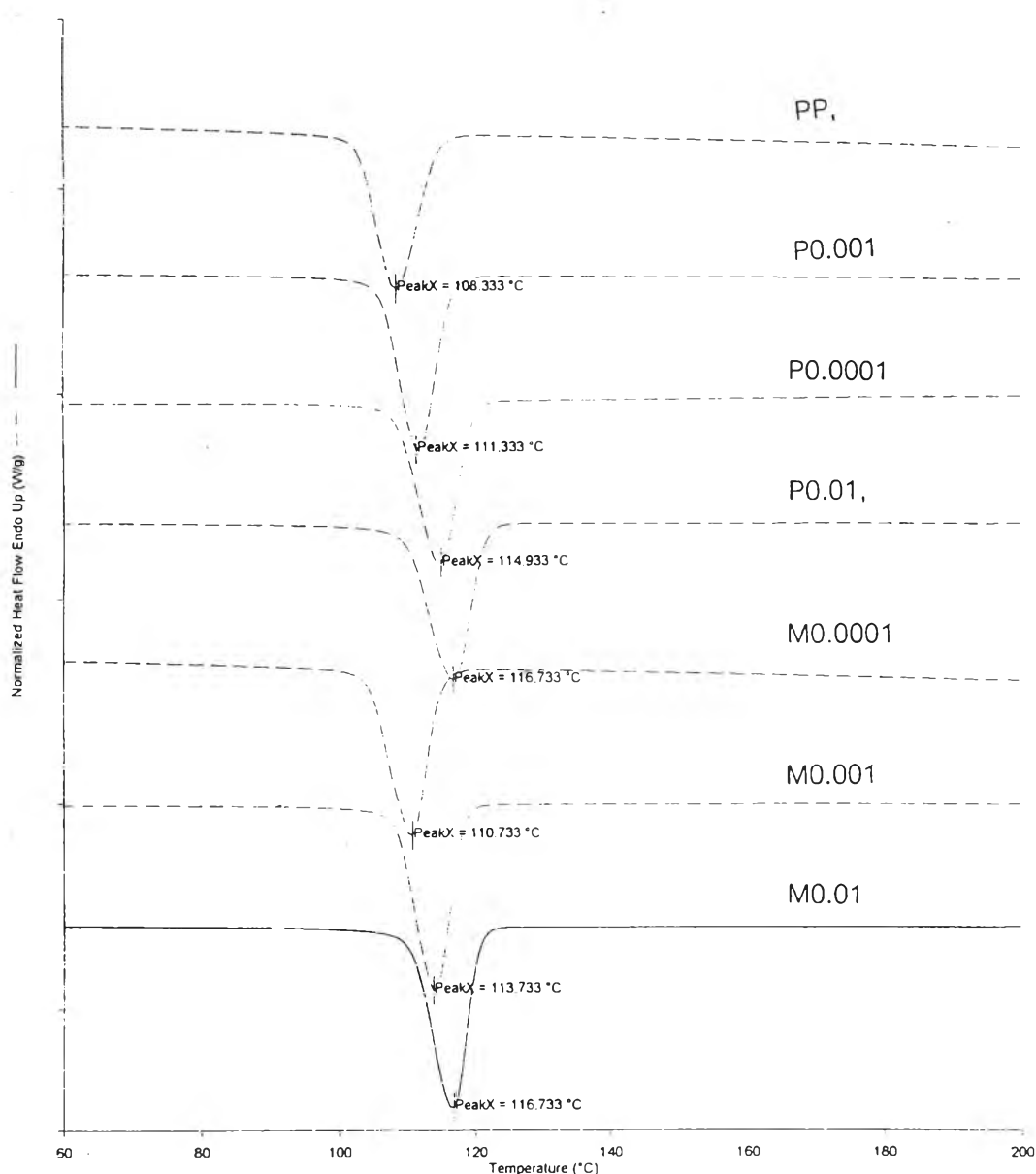


Figure 4.5 The DSC crystallization thermogram of compressed films PP, P0.0001, P0.001, P0.01, M0.0001, M0.001, M0.01

#### 4.1.2.2 Extruded films

Figures 4.6 and 4.7 are DSC melting and crystallization thermogram of PP extruded films with 0.0001 – 0.01% wt. of the E3B  $\beta$ -nucleator. This extruded films were also prepared from pelletized PP-E3B (designated M0.0001-M0.01). Based on Figure 4.6, a melting endotherm at 160°C is clearly seen in all sample types. There is, however, no melting peak of the  $\beta$ -crystalline form in PP extruded films samples (both PP-E3B and PP-masterbatch) containing E3B in the range of 0.001-0.01.

This results confirm the findings obtained from X-ray diffraction of all extruded films which reveal no diffraction characteristics of the PP  $\beta$ -crystalline form. In terms of crystallization of these extruded films (see Figure 4.7) such behavior were observed upon cooling after melting the samples using DSC. Like the findings in compressed film, the observed crystallization temperatures tend to shift to higher temperature as the E3B  $\beta$ -nucleator concentrations increased. It can be summarized that during extruded films formation, the influence of the  $\beta$ -nucleator (E3B of 0.0001-0.01 wt.% range) on  $\beta$ -phase crystalline formation of the PP is much smaller than that occurs during crystallization from the melted PP as for compressed films. It is possible that such influence of the E3B on  $\beta$ -crystalline formation in the PP extruded films may change when the higher concentration of E3B is used.



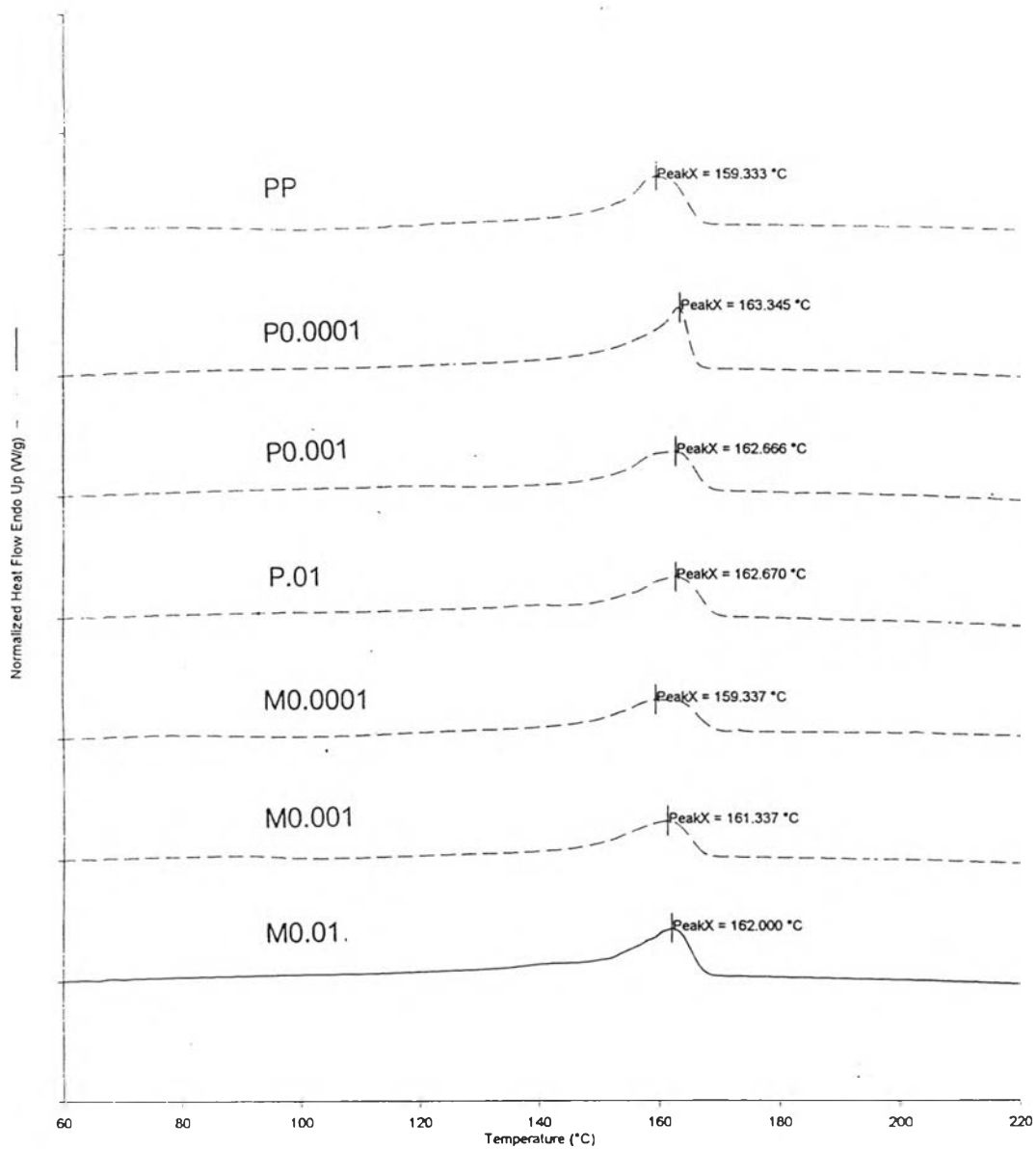


Figure 4.6 The DSC melting thermogram of extruded films PP, P0.0001, P0.001, P0.01, M0.0001, M0.001, M0.01.

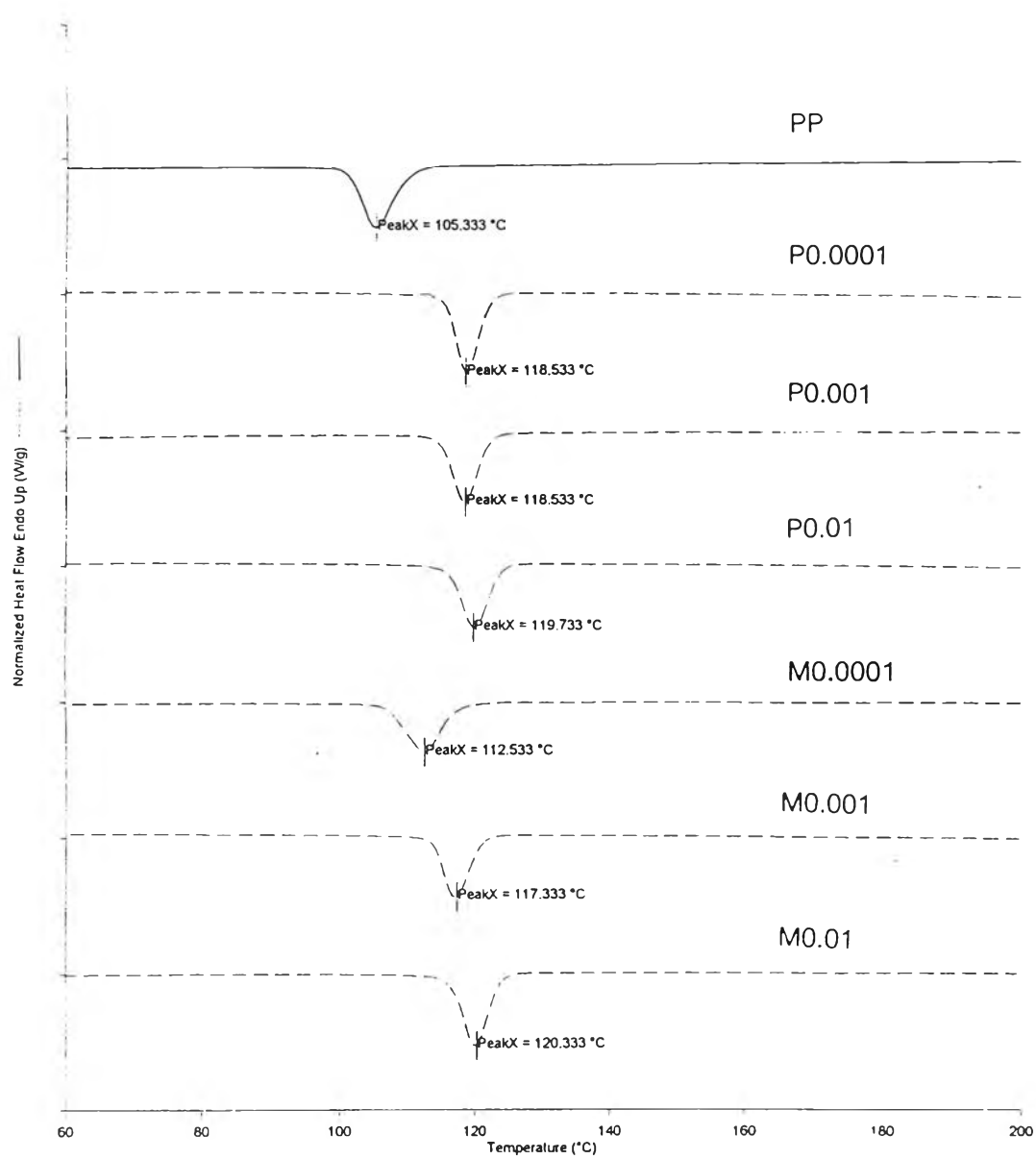
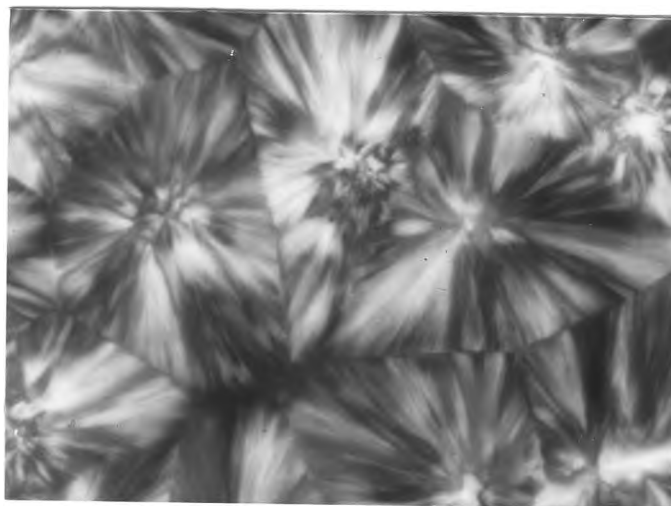


Figure 4.7 The DSC crystallization thermogram of extruded films PP, P0.0001, P0.001, P0.01, M0.0001, M0.001, M0.01

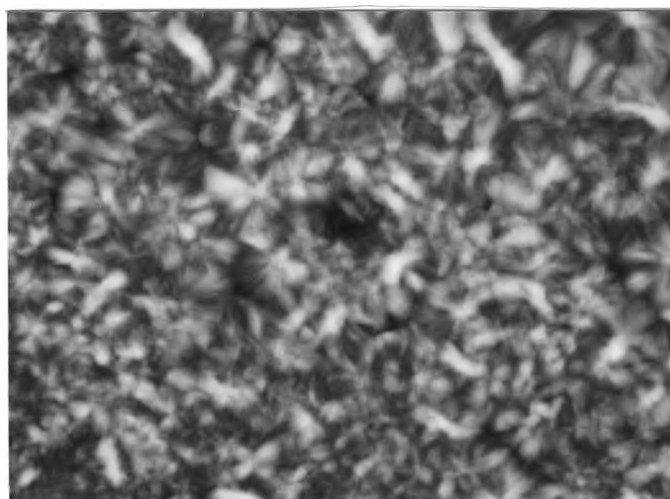
### 4.1.3 Optical polarizing microscope studies

The morphology of the  $\beta$ -phase nucleated PP was found to be distinctly different from that of the  $\alpha$  phase as revealed by optical polarizing microscopy. Figures 4.8-4.14 indicate the typical optical micrographs obtained for pure PP and PP containing  $\beta$ -nucleator, the crystallization condition being the same in both cases and as described in section 3. As shown in Figure 4.8 it can be seen that pure PP exhibits mainly large  $\alpha$  spherulite, having amounts of tangential lamellae and branching, inside the spherulite. For the PP containing Permanent Red E3B, the morphology essentially consisted of large  $\alpha$  spherulite and small  $\beta$  spherulites. The  $\beta$  spherulite has distinctly different internal morphology, in that the  $\beta$ -spherulite (sheaf-like structure) consists of an aggregate of lamellae that radiate from central nucleus outward and is much brighter than the normal large  $\alpha$  ones. In the case of PP containing low concentration of E3B ( P0.0001, P0.001, M0.0001, M0.001 ) a combination of large  $\alpha$  spherulites with small  $\beta$  spherulites is clearly observed. A close examination of the PP-E3B ( P0.0001, P0.001 ) show that the dispersion of small  $\beta$  spherulite is poorer as compared with PP-masterbatch containing E3B of the same content ( M0.0001 and M0.001), see Figure 4.9-4.10 and 4.12-4.13. The aggregation of small  $\beta$  spherulites tend to occur sporadically in P0.0001 and P0.001 sample. When the higher amount of E3B ( 0.01% by wt ) was used, extensive small and bright  $\beta$  crystal are formed and relatively well dispersed over the sample, as seen in Figure 4.11 and 4.14. These two micrographs of P0.01 and M0.01 look relatively the same. These result indicate that both the concentration of  $\beta$  nucleator and type or degree of mixing greatly affect the dispersion of  $\beta$  crystals in the sample. Moreover, at low concentration of E3B, it seem that the  $\beta$  spherulite formation and dispersion is more dependent on the type of mixing. The results of polarizing optical microscope suggests that the internal mixing tend to become effective in promoting the good  $\beta$  spherulite dispersion than the mechanical blending especially when a low content of E3B is used. For PP with high concentration of  $\beta$  nucleator (P0.01 and M0.01 ) type of mixing has little effect on dispersion of  $\beta$  spherulite, spherulite structures of the P0.01 and M0.01 are alike.

In order to examine whether the observed bright crystals are actually  $\beta$ -form, an additional optical melting experiment of the already crystallized samples ( as seen in Figure 4.15 (A) ) was performed. The hot stage was programmed to heat the crystallized sample at a rate of  $20^{\circ}\text{C}/\text{min}$ . Any changes in morphology of the sample upon heating was observed and photographed. A record of the changes during heating of the PP-masterbatch sample (M0.0001) was shown as an example in Figure 4.15 . The bright  $\beta$ -form spherulites were melted at the temperature range of  $\sim 148^{\circ}\text{C}$ . At this temperature range, the  $\beta$  spherulites lose their birefringence whereas the large  $\alpha$  spherulites still clearly exist. These findings help confirm on PP  $\beta$ -crystal formation produced in PP-E3B and PP-masterbatch samples as well as support the results obtained from X-ray and DSC analysis. When the  $\beta$ -phase content is considered it should be noted, however, that the highest relative  $\beta$ -phase content as evident by measured  $k_x$  value is found in the P0.0001 (PP-E3B) compressed films samples, see the X-ray diffractogram results in section 4.1.1.1. If comparing P0.0001 with M0.0001, for instance, one could realize that mechanical blending of PP and E3B may not be as effective as internal mixing in dispersing the E3B  $\beta$ -nucleator, but the resulting structure of the former after pelletization gives rise to higher  $\beta$ -crystallinity content. Overall findings show relationships between  $\beta$ -phase content and  $\beta$ -crystal morphology. Dispersion of the  $\beta$ -crystal as well as their quantity, size, and perfectness may contribute to the  $\beta$ -crystallinity content in a given sample.

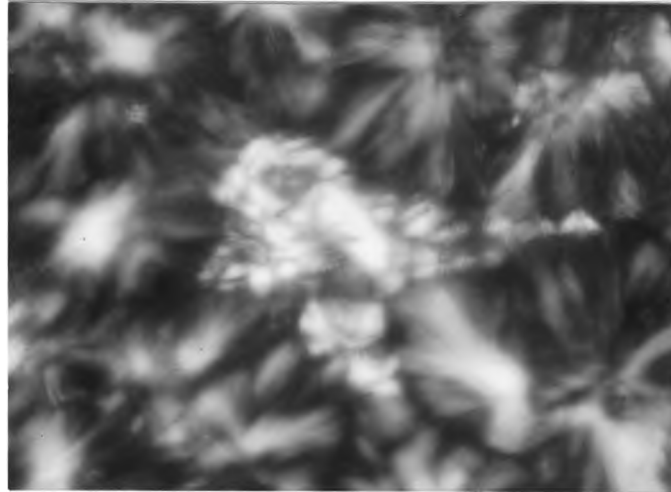


A

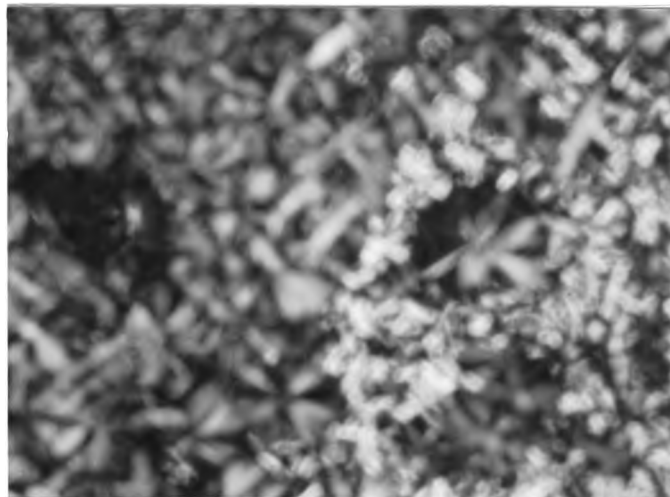


B

Figure 4.8 The optical polarizing micrographs for pure iPP. A) magnification X 500, B) magnification X 200

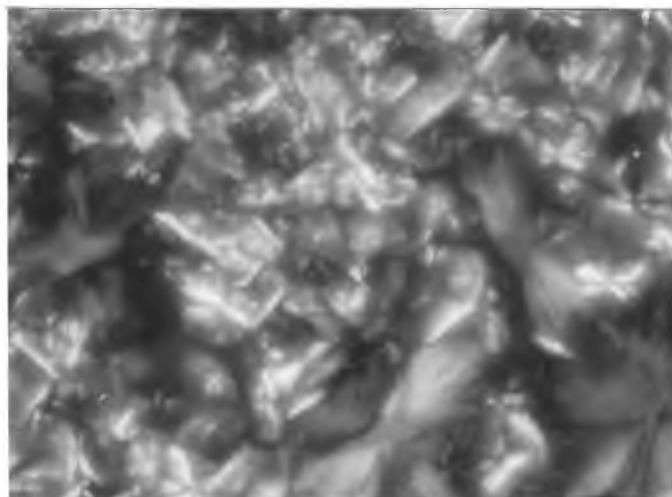


A



B

Figure 4.9 The optical polarizing micrographs for P0.0001. A) magnification X 500, B) magnification X 200

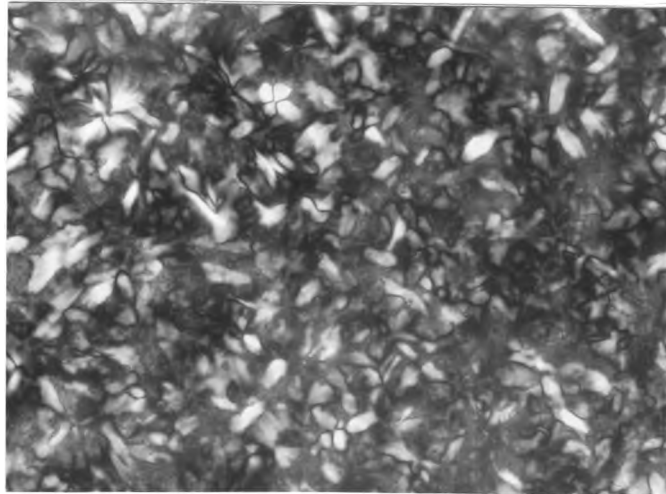


A

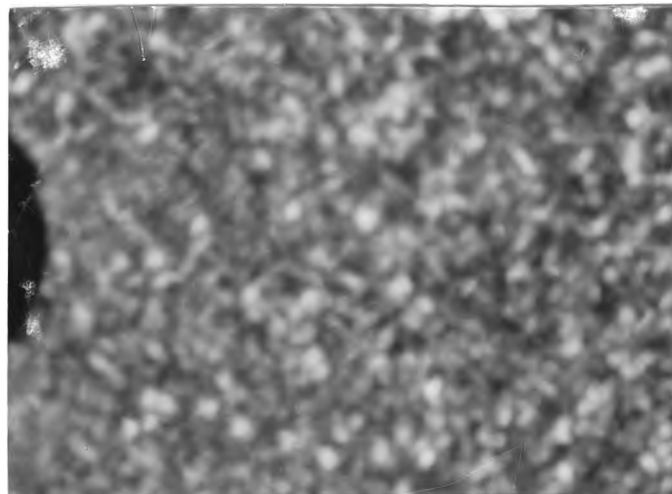


B

Figure 4.10 The optical polarizing micrographs for P0.001. A) magnification X 500, B) magnification X 200



A



B

Figure 4.11 The optical polarizing micrographs for P0.01. A) magnification X 500, B) magnification X 200



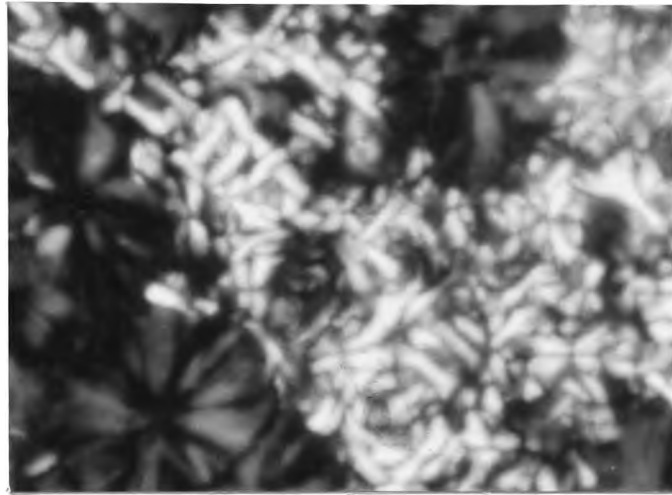


A



B

Figure 4.12 The optical polarizing micrographs for M0.0001. A) magnification X 500, B) magnification X 200

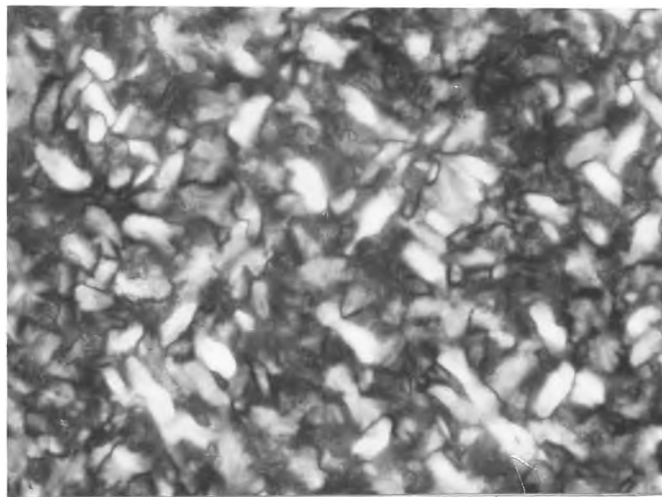


A

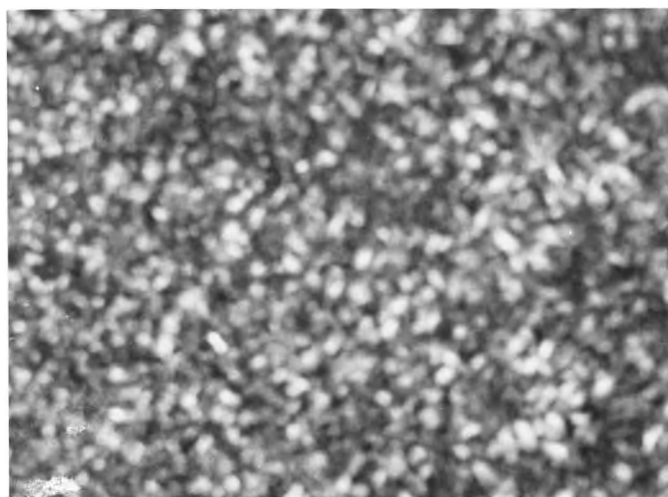


B

Figure 4.13 The optical polarizing micrographs for M0.001. A) magnification X 500, B) magnification X 200

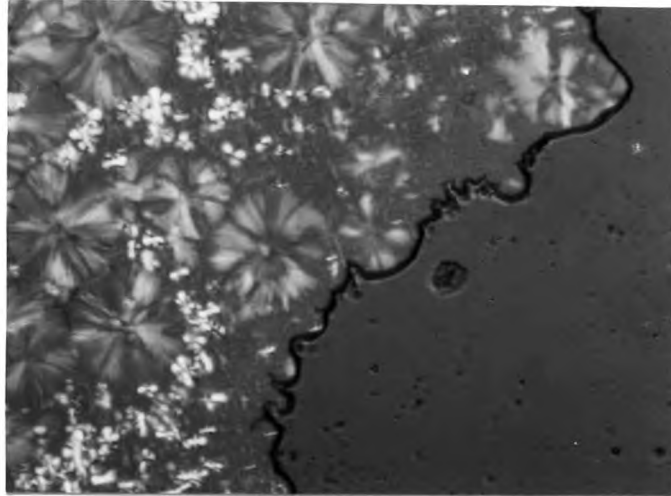


A

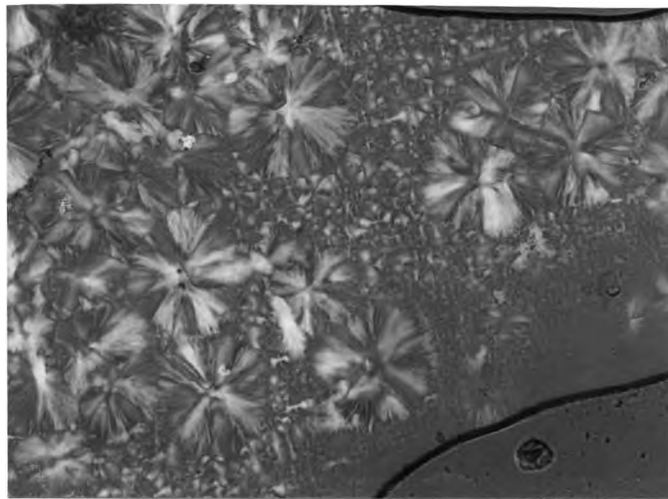


B

Figure 4.14 The optical polarizing micrographs for M0.01. A) magnification X 500, B) magnification X 200



A



B

Figure 4.15 The optical polarizing micrograph for M0.0001 A) magnification X 200 at 30°C, B) magnification X 200 at 148°C

## 4.2 Mechanical Properties Studies

### 4.2.1 Compressed films

Based on the mechanical test results, important film properties such as tensile modulus, elongation at break, toughness, and tensile strength are measured and shown in Figures 4.16-4.19. In each figure, mechanical properties of films from the pelletized PP-E3B (P0.0001-P0.01) and PP-masterbatches (M0.0001-M0.01) are compared. Since compressed films properties are basically isotropic, therefore, test specimens were randomly prepared from the compressed PP films without having taken the films direction in to account. In general, it was found that tensile strengths of pure PP and PP containing  $\beta$ -nucleator films are approximately the same within the error bar of ~20-27 MPa ( Figure4.16 ). Modulus of elasticity of  $\beta$  nucleated PP films, however, can be lower, equivalent or even higher than that of the pure PP compressed films ( see Figure 4.17 ). Films containing E3B of 0.0001% and 0.001 % by weight ( both PP-E3B and PP-masterbatch ) show lower modulus of elasticity than that of the pure PP films. For sample with 0.01% E3B, P0.01 exhibits approximately equivalent modulus value to that of PP (~350 MPa) whereas the PP-masterbatch (M0.01) sample posses the highest modulus of all films tested. The M0.01 film modulus value is ~420 MPa which is 20% higher than modulus of the pure PP film.

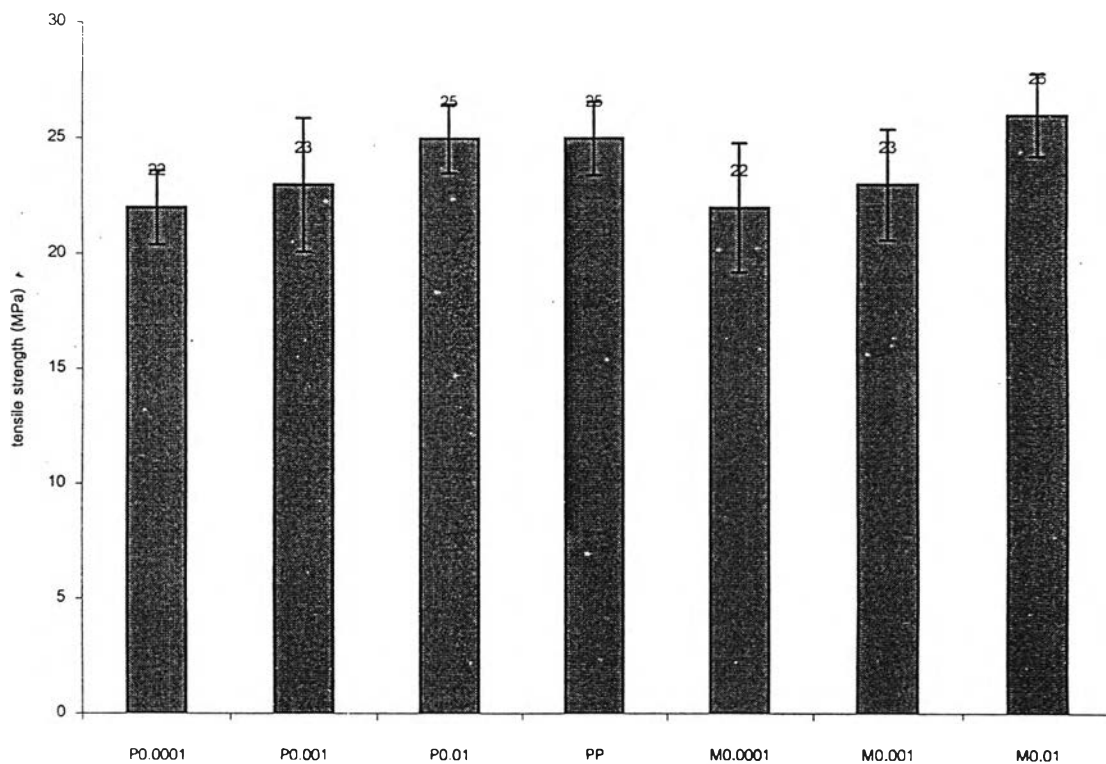


Figure 4.16 Tensile strength of compressed films

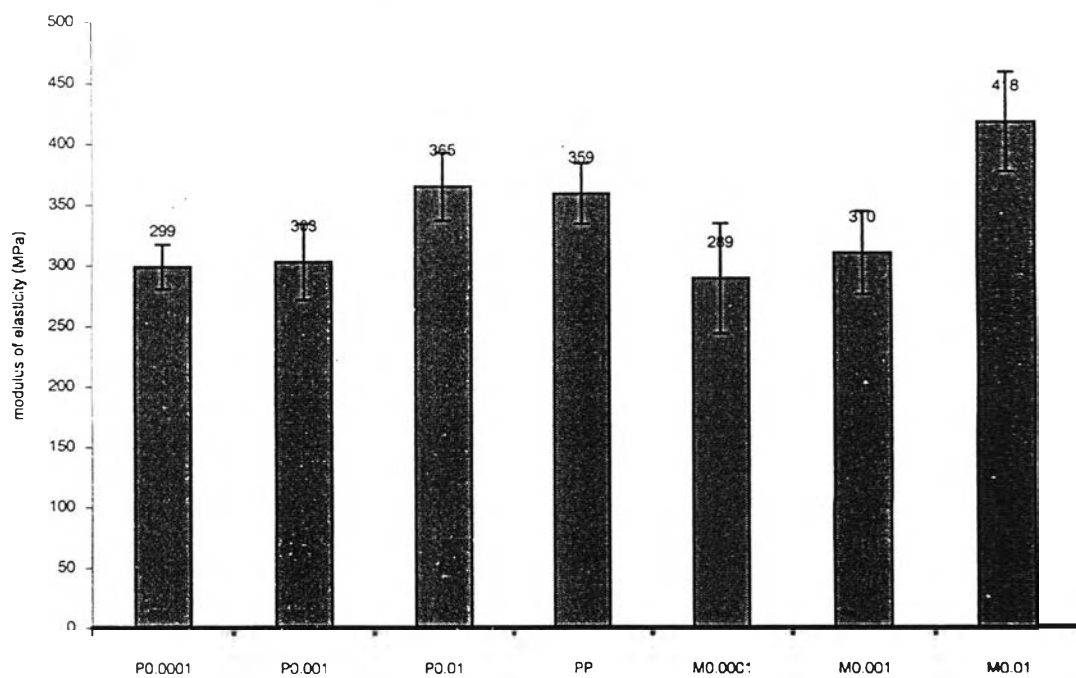


Figure 4.17 Modulus of elasticity of compressed films

In contrast to the elongation at break, PP films with 0.0001% and 0.01 % E3B exhibit nearly 100% higher in elongation at break as compared with that of the PP without  $\beta$ -nucleator ( Figure 4.18 ). The elongation at break of the compressed films of both P0.01 and M0.01 are in the range of 7-8% which is equal to the PP film property. Overall toughness results are mainly attributed by a large difference in elongation at break of all films tested. It can be seen from Figure 4.19 that all PP compressed films containing  $\beta$ -nucleator have higher toughness than the PP. Compressed films prepared from pelletized PP-Masterbatch of 0.0001% E3B (M0.0001) have the highest toughness value of ~399 MPa. The P 0.0001 and P0.001 films type exhibit very high toughness with an average of ~320 and 350 MPa, respectively. The toughness of the P0.001 as well as M0.001 and M0.01 films are more or less the same which is slightly higher than PP films' toughness value

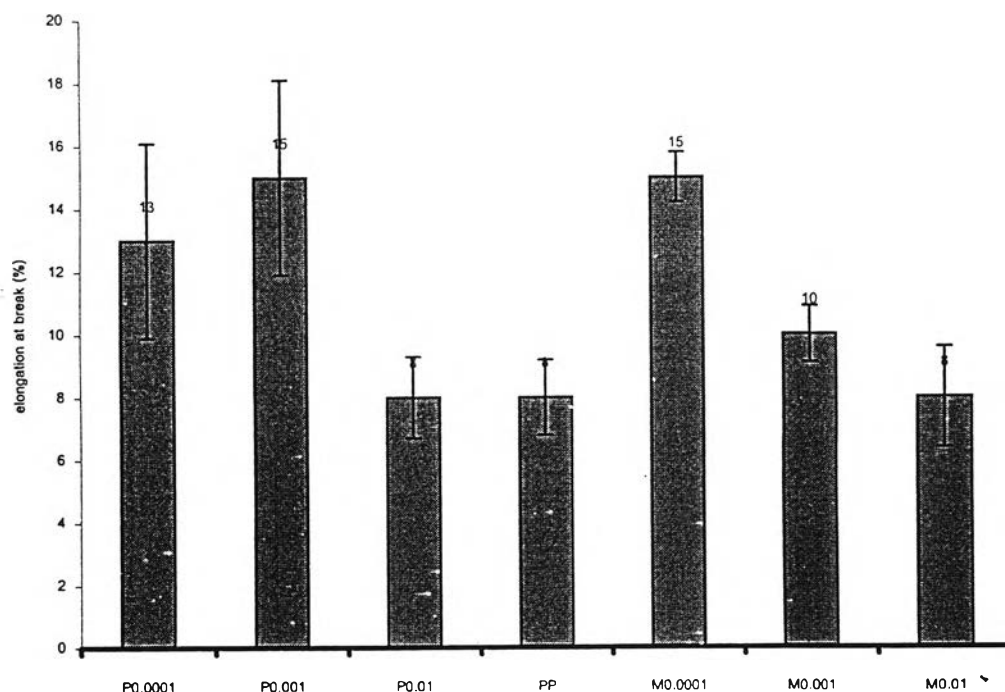


Figure 4.18 Elongation at break of compressed films

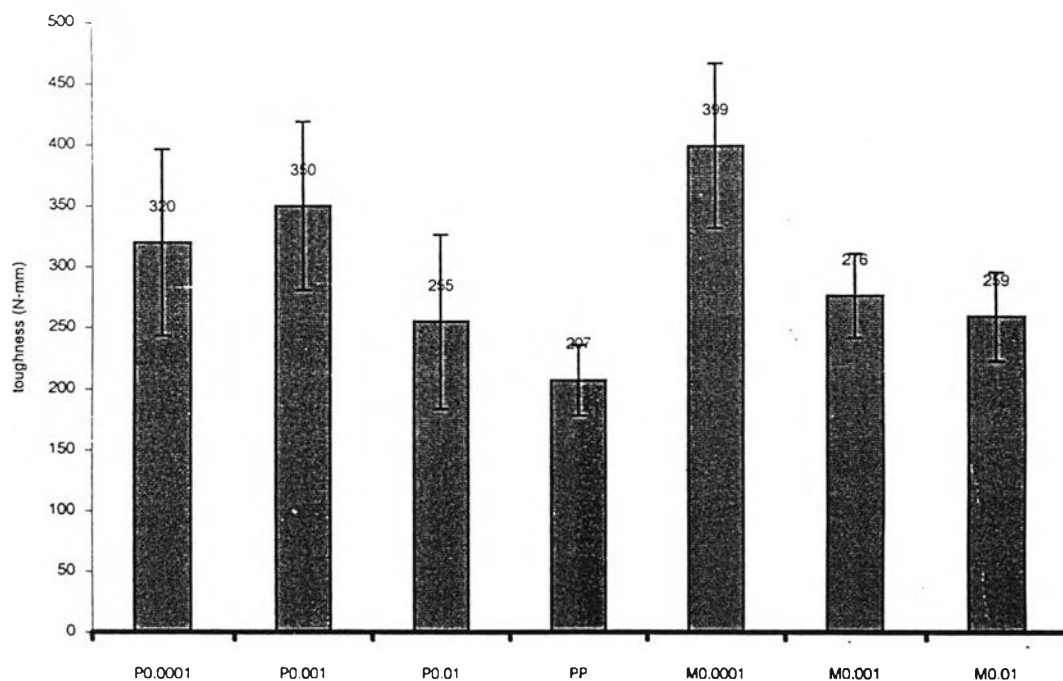


Figure 4.19 Toughness of compressed films

In order to understand what controls or affects mechanical properties of  $\beta$ -nucleated PP, it is worthwhile looking closely at the relationship between the  $\beta$ -crystalline phase content, as indicated by  $k_x$  value, and the mechanical testing result of the films. Such relationship summarized in Table 4.2.

Table 4.2 Tensile properties of compressed film and  $k_x$  value

Sample type	$k_x$ value	Modulus (MPa)	Tensile strength (MPa)	Elongation at break (%)	Toughness (N-mm)
P0.0001	0.91	299 ± 18.4	22 ± 1.6	13 ± 3.1	320 ± 76.7
P0.001	0.68	303 ± 31.3	23 ± 2.9	15 ± 3.1	350 ± 69.2
P0.01	0.55	365 ± 27.8	25 ± 1.5	8 ± 1.3	255 ± 71.4
PP	-	359 ± 24.9	25 ± 1.6	8 ± 1.2	207 ± 28.7
M0.0001	0.64	289 ± 45.5	22 ± 2.8	15 ± 0.8	399 ± 67.3
M0.001	0.72	310 ± 34.2	23 ± 2.4	10 ± 0.9	276 ± 34.5
M0.01	0.58	418 ± 40.9	26 ± 1.8	8 ± 1.6	259 ± 36.4



From Table 4.2 it is quite clear that the three samples with highest elongation at break and toughness values (P0.0001, P0.001 and M0.0001) have very high  $\beta$  phase contents and correspondingly  $k_x$  values of 0.91, 0.68 and 0.64 respectively. It was reported that  $\beta$  spherulites with a sheaf-like structure differs largely from the  $\alpha$  spherulites in that  $\beta$  spherulites consist of an aggregate of lamellae radiating from the central nucleus out ward while the tangential crystallites are commonly present in  $\alpha$  spherulites. The tangential crystals in  $\alpha$  spherulite build a rigid "cross-hatched" network which makes the amorphous component in the intercrystalline zone much more difficult to deform. Furthermore, this interlock crystalline structure stiffens the  $\alpha$  spherulite considerably. Accordingly, films having higher  $\beta$  phase content should also have greater deformability and possibly lower modulus. The above principles seem to apply well to the overall observations in this study.

The films exhibiting low modulus, high elongation at break, and high toughness of the  $\beta$  nucleated films also posses high  $\beta$  phase content ranging from  $\sim 0.64 - 0.9$  (as for P0.0001, P0.001, M0.0001, and M0.001 samples). Thus the combined effect of the unique features of  $\alpha$  and  $\beta$  spherulites and their relative crystal contents in the compressed film can play an important role in controlling properties of the film.

#### 4.2.2 Extruded film

Figures 4.20-4.23 show comparison of mechanical properties for extruded films of pure PP and PP containing E3B  $\beta$ -nucleator (both P0.0001 – P0.01 and M0.0001 – M 0.01). The modulus, tensile strength, elongation at break and toughness values of the film's machine direction (MD) are reported versus the transverse direction (TD) properties.

Mechanical properties of the produced extruded films are essentially anisotropic. Films tensile strengths, elongation at break and toughness in machine direction (MD) are much higher than those in transverse direction (TD), see Figure 4.20-4.22. However, modulus of the extruded films of PP and PP with E3B nucleator ( 0.0001-0.01%) show slight differences between MD and TD modulus values.

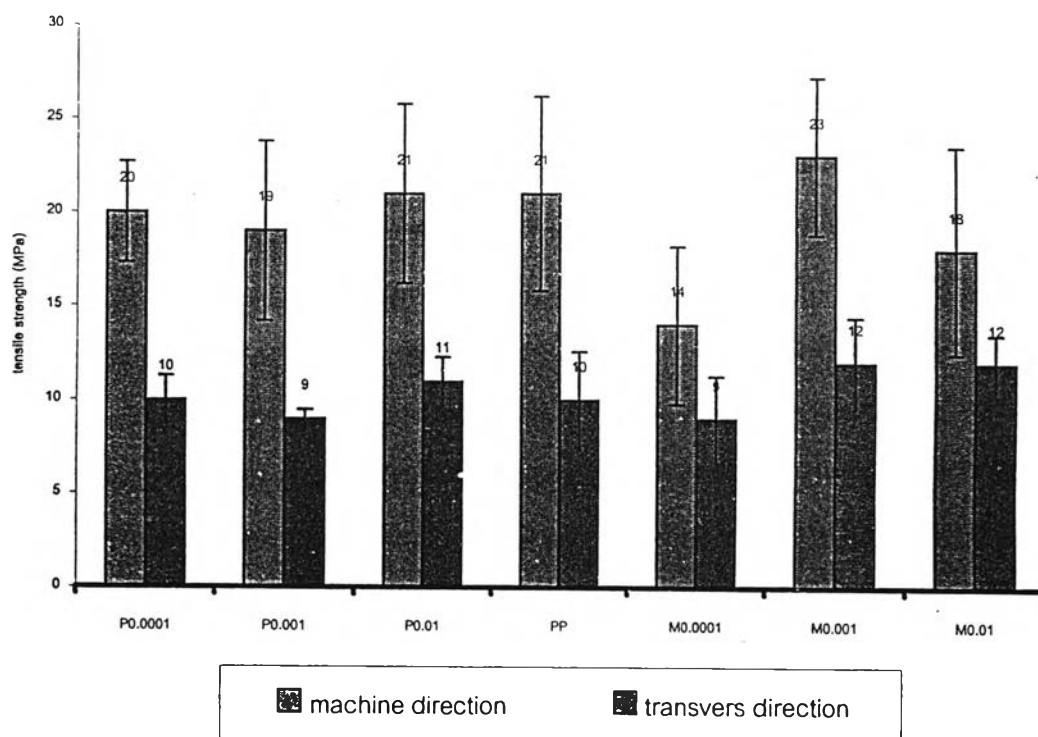


Figure 4.20 Tensile strength in machine and transverse directions of extruded

films

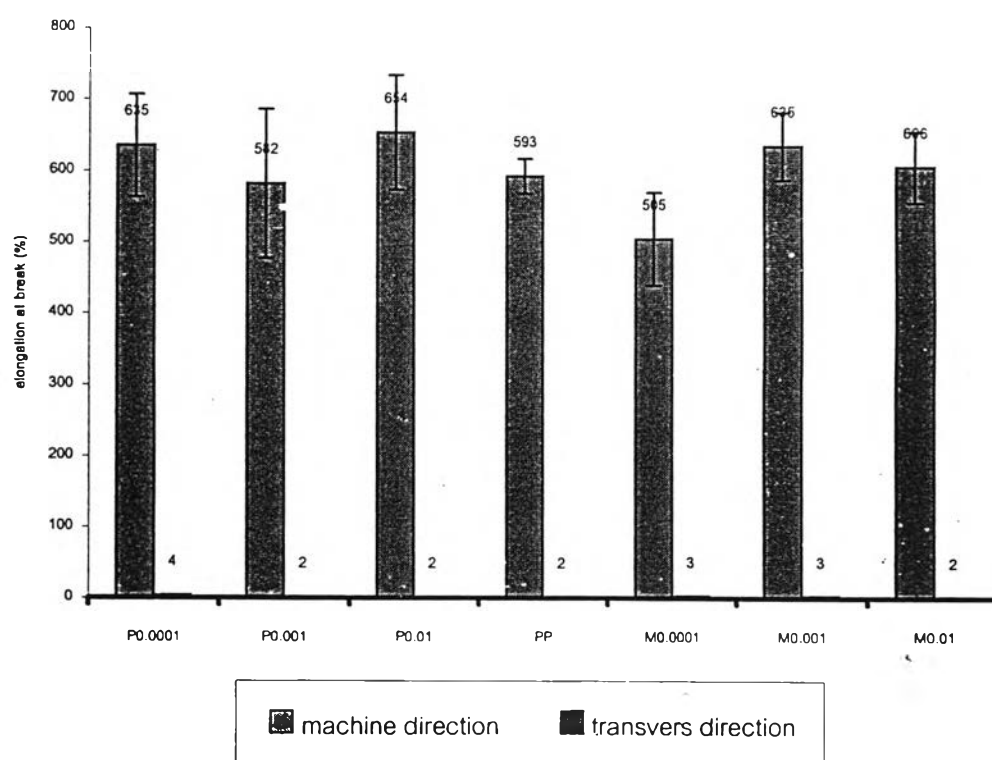


Figure 4.21 Elongation at break in machine and transverse directions of extruded films

It can be noticed that the pure PP and PP with low E3B concentration (P0.0001 and M0.0001) have similar modulus properties and average MD modulus values (~706-719 MPa) are higher than average TD values (~583-623 MPa). With an increase % E3B, the TD modulus tends to increase while MD modulus is relatively unchanged. As seen in P0.01, M0.001 and M0.01 samples, the TD modulus values become slightly higher than the MD modulus.

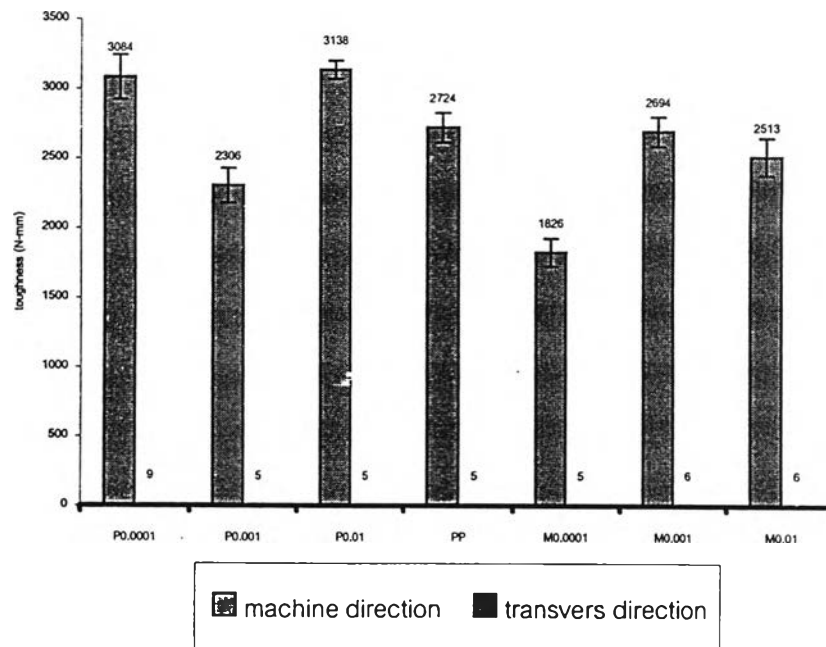


Figure 4.22 Toughness in machine and transverse directions of extruded films

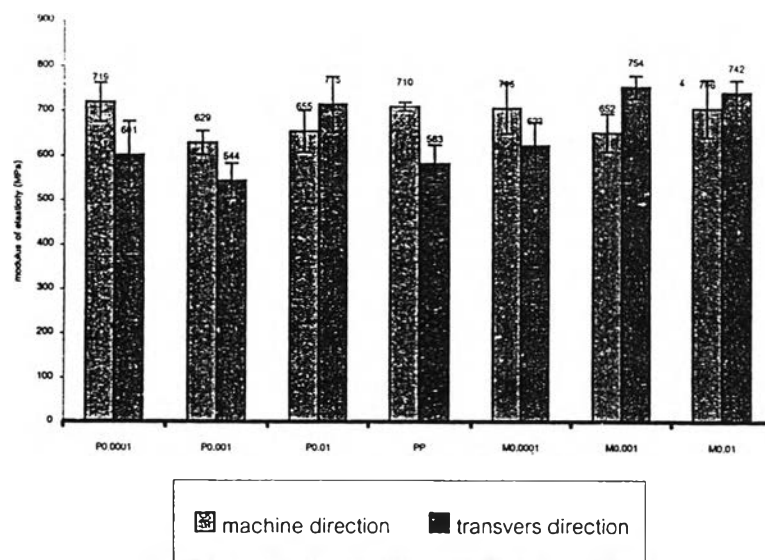


Figure 4.23 modulus of elasticity in machine and transverse directions of extruded films

In case of tensile strengths, elongation at break, and toughness, analysis and discussion are made based on MD properties of the extruded films because the TD values are much lower and there is no significant changes in TD as a function of E3B content. Most PP extruded films containing E3B possess comparable MD tensile strengths with the pure PP. Only the M0.0001 and M0.01 films tend to show a decrease in MD tensile strengths as compared with the PP sample. A decrease in tensile strength of PP containing E3B  $\beta$ -nucleator may be attributed to the influence of the localized stress caused by pigment, which could lead to the formation of voids. Similar effect was also reported during fiber formation of PP coloured with quinacridone. Due to the localized stress caused by pigment, voids could stretch perpendicularly to the fiber axis to lateral slot which, in turn, lead to a decrease in fiber strength.<sup>57</sup> With regard to elongation at break and toughness, a slight increase in the average elongation at break of the P0.0001 and P0.01 extruded films is noticed, and these changes tend to influence an overall increase in film toughness of P0.0001 and P0.001 as compared with pure PP films. The two PP-masterbatch films (M0.001 and M0.01) show approximately equivalent film toughness to pure PP. A large decrease in toughness is observed in PP-0.001%E3B (P0.001) and PP-masterbatch (M0.0001).

Overall results reveal that mechanical properties of extruded films prepared from the pelletized PP-3B and from PP-masterbatches are different. Tougher films compared with pure PP can be produced from PP containing E3B of 0.0001% and 0.01% (P0.0001 and P0.01) which was mechanically blended prior to pelletization. The M0.0001 – M0.01 type samples which were prepared from PP-masterbatch tend to show lower toughness than the P0.0001 – P0.01 samples. When the tensile behaviors of these extruded films are closely examined, it can be seen as in Figures 4.25-4.26 that the P0.0001 and P0.01 films break at higher %strain than the PP films (Figure 4.24). For PP, the film was stretched and at ~500% strain, molecular chains become more restricted to deformation. This phenomenon, as known as "strain hardening", gives rise to an increase in stress upon further stretch on deformation. However it is noticeable in the case of PP with 0.0001 and 0.01 %E3B (P0.0001 and P0.01) that the strain hardening starts at lower % strain (<500%) than that observed in the PP. Such difference in deformability of the pure PP and PP containing E3B are also partly responsible for different films toughness.

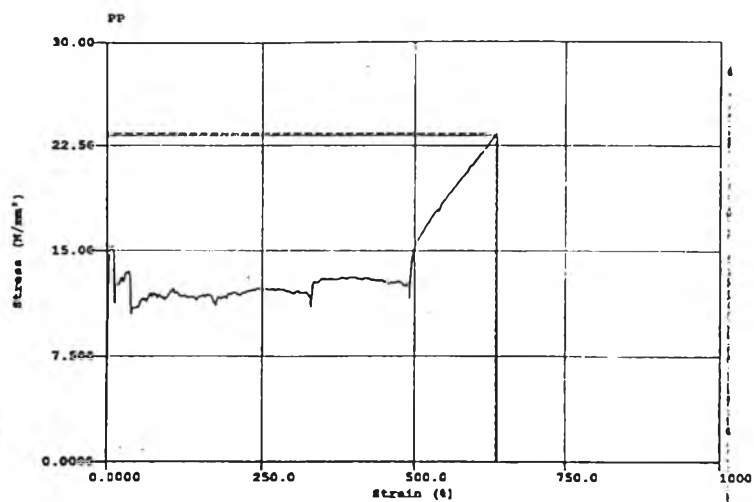


Figure 4.24 Tensile behavior of PP extruded films in machine direction

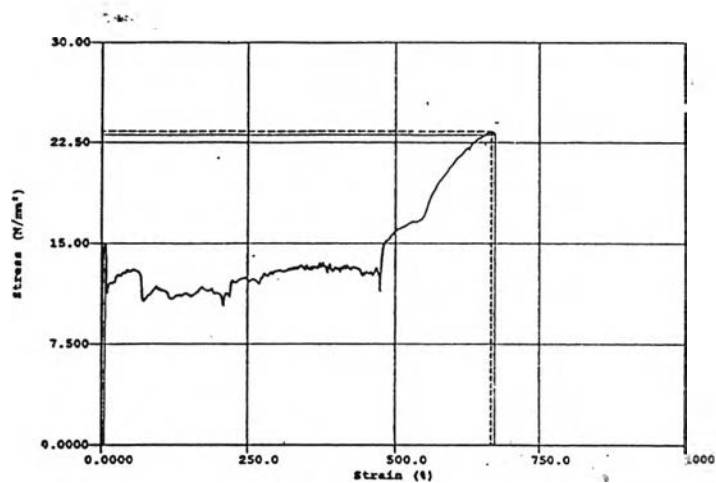


Figure 4.25 Tensile behavior of P0.0001 extruded films in machine direction

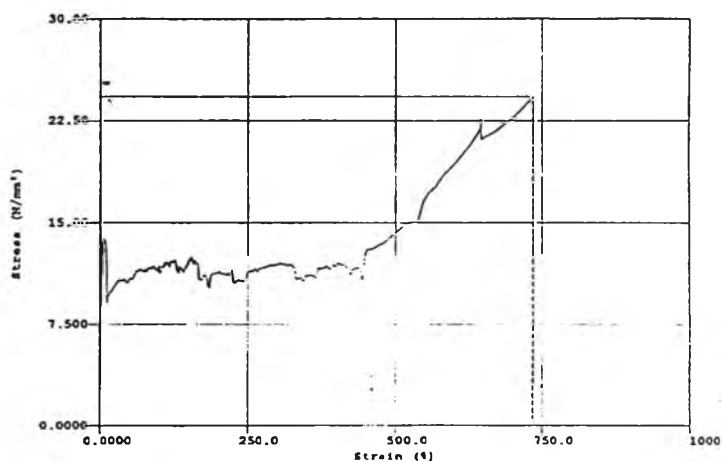


Figure 4.26 Tensile behavior of P0.01 extruded films in machine direction

The reason why the P0.0001 and P0.01 films toughness are higher than the PP film should be attributed to and inclusion of E3B or pigment in the PP molecular structure. The presence and location of E3B may affect the molecular orientation during stretch or drawing, however, a clear picture of such effect in extruded film of PP-E3B has not been achieved in this study. It has been previously reported that the phenomenon of pigments dimensions comparable to thickness of fibrils occur in location of interfibrillar zone. Thus this phenomenon is affect on the fibrillation process of the PP fibers. During fiber drawing, fibrillation process of the PP fibers processed easily because of the low interfibrillar cohesion as a result of a small amount of connecting macromolecules and weak interfibrillar bonding.<sup>57</sup>

According to the X-ray results, all PP extruded films showed neither  $\alpha$  nor  $\beta$ -diffractions, instead the smectic form as indicated by 14.8 and 21.1 diffraction angle ( $2\theta$ ) This observation implies that a presence of a small amount of E3B in a range of 0.0001-0.01% by weight may not generate the formation of  $\beta$ -crystals in PP or otherwise a so much low content of  $\beta$ -crystal may be generated but cannot be revealed by the X-ray analysis used in this study. In other words, during extruded film formation, the influence of pigments of molecular structure of crystallizable PP is much smaller than during the crystallization from the melt or as seen in compressed films. However, the extruded films of PP with E3B should have partially ordered structure of macromolecules as characterized by smectic form.

#### 4.3 Oxygen Permeation measurement.

In this study, a preliminary result on gas permeability or porosity of pure PP and PP with  $\beta$ -phase was obtained by  $O_2$  permeation measurement. Compressed and extruded films of pure PP and P 0.0001 were tested and compared. The P0.0001 film was selected as the compressed film of PP-0.0001% E3B posses the highest  $\beta$ -phase content ( $k_x \sim 0.91$ ).

Based on Figure 4.27, both PP and P.0001 extruded films have higher permeation than compressed films. Permeation performances of P0.0001 extruded films could be

diffractogram possesses density of  $\approx 0.88 \text{ g/cm}^3$  while densities of  $\beta$  and  $\alpha$ -iPP crystals are reported to be  $\sim 0.921$  and  $0.946 \text{ g/cm}^3$ , respectively. Thus, the PP and P 0.0001 cast films in smectic structure appear to be less dense than both  $\alpha$ -PP and 90%  $\beta$ -iPP (P0.0001) compressed films.

However, for PP and P0.0001 extruded films, it is possible that pigment in P 0.0001 may locate in intermolecular chains or interfibrillar zone as reported by Broda<sup>57</sup>. The presence of pigment in the PP structure may somehow limit volume contraction during film formation, resulting in less dense or more porous film as compared to the pure PP. In order to better understand a mechanism involved in porous PP film produced by an incorporation of pigment such as E3B in this case, a further investigation needs to be carried out. In summary, current observations are interesting and could be useful for further study of porous fiber formation or film application in plastic packaging selective membrane and filter technology.

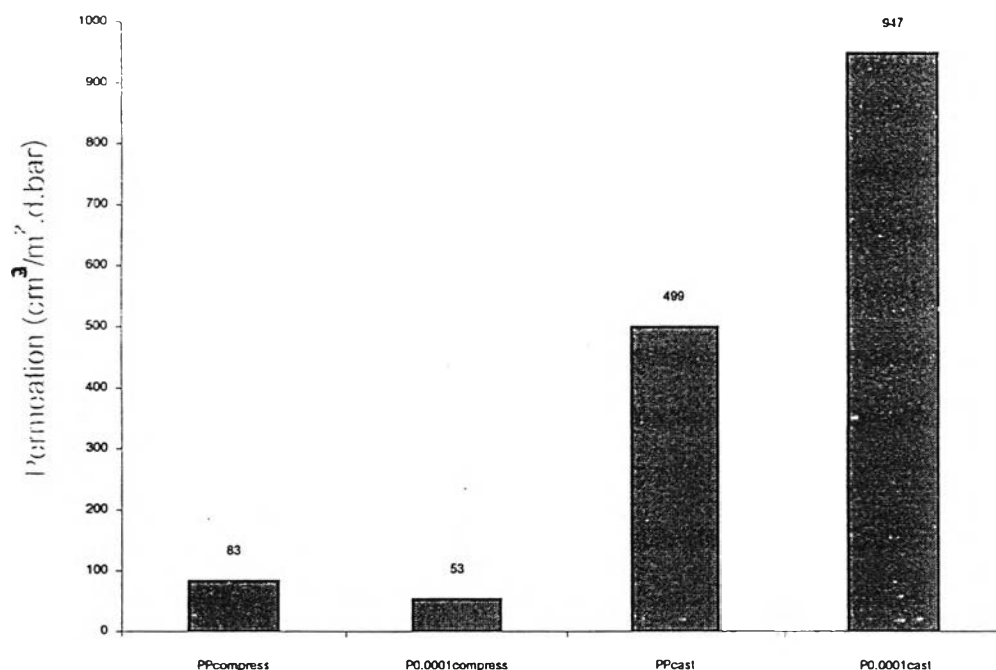


Figure 4.27 Oxygen permeation of compressed and extruded films